Journal of Catalysis **191,** 354–363 (2000)
doi:10.1006/jcat.1999.2767, available online at http://www.idealibrary.com on IDEAL®

An FT-IR and Reactor Study of the Dehydrochlorination Activity of $CuCl_2/\gamma$-Al_2O_3-Based Oxychlorination Catalysts

D. Carmello,* E. Finocchio,† A. Marsella,* B. Cremaschi,* G. Leofanti,*,[1] M. Padovan,*,[2] and G. Busca†

*EVC Italia, Inovyl Technology Centre, Via della Chimica 5, 30175 Porto Marghera, Venezia, Italy; and †Dipartimento di Ingegneria Chimica e di Processo, Università di Genova, P.le J. F. Kennedy, I-16129 Genova, Italy
E-mail: diego_carmello@evc-int.com

Received August 9, 1999; revised November 4, 1999; accepted November 24, 1999

The conversion of ethylchloride into ethylene + HCl on pure and doped alumina supports and on $CuCl_2$–Al_2O_3-based oxychlorination catalysts has been investigated by pulse reactor and FT-IR spectroscopy. FT-IR spectra of ethylchloride adsorbed on γ-Al_2O_3 show weakly molecularly adsorbed species and ethoxy groups formed by nucleophilic substitution. Additionally, adsorbed diethylether is also observed. The analysis of the gas-phase species shows that ethoxy groups decompose, giving rise to ethylene at 523 K. Under the same conditions, gaseous HCl is also released from the surface and diethylether is also observed in the gas phase. Chlorination of alumina with HCl only partially hinders the dehydrochlorination mechanism occurring through ethoxy groups. Experiments performed on alumina doped with $MgCl_2$ and KCl indicate that the site reactivity scale for EtCl conversion to ethylene is the following: bare Al_2O_3 > $CuCl_2$ on Al_2O_3 > $MgCl_2$ on Al_2O_3 > KCl on Al_2O_3. Doping with $MgCl_2$ and in particular with KCl limits the activity of the bare support in the dehydrochlorination. These data strongly support the previous proposal that the exposed alumina surface catalyzes the dehydrochlorination of EDC to VCM, with a consequent loss in selectivity in the oxychlorination reactor. The beneficial effect of doping with KCl and $MgCl_2$ is due to the reduced dehydrochlorination activity.

INTRODUCTION

The heterogeneously catalyzed gas-phase oxychlorination of ethylene to 1,2-dichloro-ethane (ethylene dichloride, EDC),

$$H_2C{=}CH_2 + 2\,HCl + \tfrac{1}{2}\,O_2 \rightarrow Cl{-}CH_2{-}CH_2{-}Cl + H_2O,$$

followed by the dehydrochlorination of EDC represents the main way for the production of vinyl chloride monomer (VCM) and of its polymer polyvinyl chloride (PVC) (1, 2). The catalysts currently used are based on $CuCl_2$ supported on alumina and doped with other metal chlorides such as $MgCl_2$ and KCl, for fixed bed and fluidized bed technology, respectively. The selectivity obtained for this process is very high, but not negligible amounts of by-products, namely 1,1,2-trichloroethane, carbon tetrachloride, chloroform, chloral, and ethylchloride are reported to be formed (1, 2).

In a recent paper (3) we investigated this catalytic system and we provided evidence for a negative role of uncovered γ-Al_2O_3 surface, considered to be responsible for the dehydrochlorination of EDC to VCM in the oxychlorination reactor. Further oxychlorination of VCM in the reactor would produce the main by-product 1,1,2-trichloroethane. This compound can undergo further dehydrochlorination–oxychlorination giving rise to other by-products. This would be a main cause of loss of selectivity to EDC.

To have more information on the supposed negative role of uncovered alumina, favoring the unwanted dehydrochlorination reaction, we investigated the adsorption and the conversion of ethylchloride (EtCl) on both pure and KCl- and $MgCl_2$-doped γ-Al_2O_3, on KCl- and $MgCl_2$-doped $CuCl_2/\gamma$-Al_2O_3, and on $CuCl_2/\gamma$-Al_2O_3 oxychlorination catalysts. EtCl has been chosen as the simplest chlorinated probe molecule that can give dehydrochlorination reaction with the purpose to investigate the reaction mechanisms over these catalysts. We followed the reaction of EtCl in a static IR cell, looking at the spectra of both surface and gaseous species, as described previously (4). We also compared these data with those we obtained using a conventional pulse reactor system. In the text some results concerning oxygenate compounds interaction with the catalyst are also proposed. The study of the interaction of these compounds with the catalysts is needed to identify some surface species and some features of the surface pathways.

EXPERIMENTAL

γ-Al_2O_3 was a commercial sample from Condea (surface area, 174 m^2/g; pore volume, 0.50 cm^3/g). The

[1] Present address: Via Firenze 43-20010 Canegrate, MI, Italy.
[2] Present address: Via Villa Mirabello 1-20125 Milano, Italy.

0021-9517/00 $35.00

TABLE 1

Characteristics of the Samples under Study

Sample notation	Composition[a]	Surface area (m^2/g)	Theoretical monolayer fraction
A	γ-Al_2O_3	174	0.00
1 CuClA	1% Cu/γ-Al_2O_3	188	0.09
5 CuClA	5% Cu/γ-Al_2O_3	154	0.50
9 CuClA	9% Cu/γ-Al_2O_3	117	0.99
KA	2.8% K/γ-Al_2O_3	140	
MgA	1.7% Mg/γ-Al_2O_3	160	
KCuA	2.8% K-5% Cu/γ-Al_2O_3	130	
MgCuA	1.7% Mg–5% Cu/γ-Al_2O_3	165	

[a] %, metal amount w/w.

oxychlorination catalysts were prepared by incipient wetness impregnation of γ-Al_2O_3, with $CuCl_2$ 2 H_2O, KCl, and $MgCl_2 \cdot 6\ H_2O$. After impregnation, all samples were dried at 393 K for 2 h. A summary of the samples under study is reported in Table 1.

FT-IR spectra have been recorded with a Nicolet Magna 750 instrument, using conventional IR cells with NaCl windows, connected to an evacuation/gas manipulation apparatus. The sample powders were pressed into self-supporting disks and outgassed (10^{-4} Torr, 1 Torr equal to 133.3 Pa) at 523 K for 20 min before the interaction experiments. For pure γ-Al_2O_3, outgassing at 923 K has also been performed before some experiments in order to have a largely dehydroxylated surface.

Surface area was calculated by BET method using a Micromeritics ASAP 2010 apparatus. Catalytic reactivity tests have been carried out on a pulse microreactor system as described previously (3). The reactants were injected in the microreactor with the following sequence: ethylchloride, HCl, and oxygen at 503 and 523 K. The injection of HCl and oxygen is required in order to avoid catalyst deactivation (reduction) due to the oxychlorination reaction that is carried out at the expense of the formed ethylene.

RESULTS

1. *By-Products in the Industrial Plant Ethylene Oxychlorination Process*

In Table 2 a list of the main by-products and their typical percent selectivities found in industrial ethylene oxychlorination plants (EVC processes) are reported. The main by-products are carbon dioxide and carbon monoxide: the first is thought to come mainly from the catalytic oxidation of ethylene and the second from the decomposition of oxygenated organic compounds. The key side reaction leading to the formation of nearly all the organic by-products appear to be the dehydrochlorination of 1,2-dichloroethane to vinyl chloride: under the oxychlorination conditions

TABLE 2

Main By-Products Percentage Molar Yields in the Oxygen-Based Ethylene Oxychlorination Industrial Plants

By-Products	Fixed bed technology	Fluid bed technology
$CO_2 + CO$	0.5–0.7	1–2
1,1,2-Trichloroethane	0.1–0.3	0.3–0.8
Trichloroacetaldehyde	0.3–0.5	0.1–0.3
Trichloromethane	0.1–0.2	0.1–0.2
Tetrachloromethane	0.1–0.2	0.1–0.2
Dichloroethylenes	<0.1	<0.1

vinyl chloride reacts to form 1,1,2-trichloroethane. That compound undergoes further dehydrochlorination leading to dichloroethylenes and (through a path still not understood) to trichloroacetaldehyde. Furthermore, this last compound can be decomposed to trichloromethane and tetrachloromethane. Therefore understanding the first step of that reaction chain should make it possible to control and minimize the formation of organic by-products increasing the raw material yields and minimizing the environmental impact of the plants.

2. *A Pulse Reactor Study of the Conversion of Ethylchloride (EtCl)*

The results of pulse catalytic tests are reported in Table 3. Pure alumina is the most active catalyst in the dehydrochlorination reaction, as expected. The addition of 1% copper (as $CuCl_2$) results in an evident decrease of the ethylchloride conversion to ethylene. By increasing the copper content up to 9% the activity slightly decreases again, but, if calculated on the surface area basis, the conversion is almost the same for the three Cu containing samples. On the other hand doping of alumina with K and Mg chloride also causes the decreasing of the EtCl conversion activity.

TABLE 3

Ethylchloride Conversion to Ethylene in Pulse Catalytic Experiments

	EtCl conv.%		EtCl conv. per surface unit ($\% \cdot g/m^2$)	
Catalyst	503 K	523 K	503 K	523 K
Al_2O_3	20.8	62.2	0.12	0.36
KA	4.6	7.8	0.033	0.056
MgA	5.6	—	0.035	—
1 CuA	8.2	19.8	0.04	0.1
5 CuA	7.6	20.3	0.05	0.1
9 CuA	5.1	14.4	0.04	0.1
KCuA	1.0	3.3	0.008	0.025
MgCuA	5.1	11.5	0.03	0.07

The KCuA sample shows a minimum activity in coverting ethylchloride, a "negative synergetic" effect appearing by adding K to Cu. In the case of MgCuA sample we observe a smaller decrease of the activity in ethylchloride conversion with respect to the KCuA. If we take again into account the conversion on surface area basis, it is evident that doping with KCl strongly limits the conversion of ethylchloride but also $MgCl_2$ causes a slight decrease of the catalytic dehydrochlorination activity.

3. *Interaction and Conversion of EtCl on γ-Al_2O_3: An in Situ IR Study*

The conversion of EtCl on γ-Al_2O_3 has been investigated under static conditions, into the IR cell, with monitoring the IR spectra of both adsorbed and gas-phase species. The alumina sample, after outgassing (10^{-4} Torr) at 573 K was put into contact with EtCl vapor (10 Torr), and later heated progressively in this atmosphere.

3.1. Analysis of the gas phase. In Fig. 1 the spectra of the gas phase recorded when the catalyst is progressively heated in contact with EtCl are reported. The spectra have a common absorbance scale.

Up to 523 K only the typical absorptions of EtCl gas (5), as summarized in Table 4, are found. In particular, we note the bands at 1448 and 1388 cm^{-1} (deformations of the CH_3 and CH_2 groups) and the bands with the typical PQR rotovibrational contour centered at 1289 (CH_2 wagging), 970 (C–C stretching), and 670 cm^{-1} (C–Cl stretching). At 473 K a weak new band at 1146 cm^{-1} appears. This band grows up to 523 K but disappears at 573 K. This band has been assigned to diethylether and will be discussed in the following paragraphs.

After heating at 573 K the gas-phase spectrum is definitely modified. The EtCl bands at 1289, 1250, and 975 cm^{-1} are definitely weakened, while new bands appear at 950 cm^{-1} (sharp and strong), 1420 cm^{-1}, and 1889 cm^{-1}, corresponding to the strongest IR-active modes of gaseous ethylene (namely, the fundamental wagging and scissoring modes, wCH_2, δCH_2, and the first overtone $2\,wCH_2$, respectively (6)). These bands further increase in intensity after 40 min at 573 K while at 623 K they are the only bands observed. Only traces of the bands of EtCl gas can be found and also the previously cited band at 1146 cm^{-1}, is totally disappeared.

Also in the C–H stretching region (Fig. 1, left) the gas-phase spectra are strongly modified at 573 K: bands with rotovibrational contours are observed at 3120 cm^{-1} ($\nu_{as}CH_2$), 3079 cm^{-1}, (combination), and at 2989 cm^{-1} ($\nu_{sim}CH_2$), typical of gaseous ethylene.

At 573 K, in parallel with the appearance of the ethylene bands, also the typical sharp peaks due to the rotovibrational contour of the HCl stretching of gaseous hydrochloric acid appear (sharp rotovibrational features in the range 2900–2700 cm^{-1} (7)).

3.2. Analysis of the adsorbed species on the catalyst surface. In Fig. 2 the subtraction spectra ([sample in contact with the gas] − [activated sample]) showing the bands due to the adsorbed species observed upon the experiment detailed above are reported.

At room temperature the spectrum of adsorbed EtCl can be observed. These bands are summarized and assigned in Table 4. After heating above 423 K a complex absorption in the region 1200–1000 cm^{-1} grows progressively up to 523 K. These bands are centered at 1192 (weak), 1167, 1151 (weak), 1103, and 1073 cm^{-1} and can be attributed to the C–C and C–O stretchings of alkoxy groups (8, 9). These bands, which are associated to the CH_3 deformation modes at 1447 and 1388 cm^{-1}, disappear at 573 K, just when we start to detect ethylene in the gas phase. In the same range the bands of adsorbed EtCl are also fully disappeared.

The spectra recorded after treating at temperatures higher than 573 K show bands due to a new adsorbed

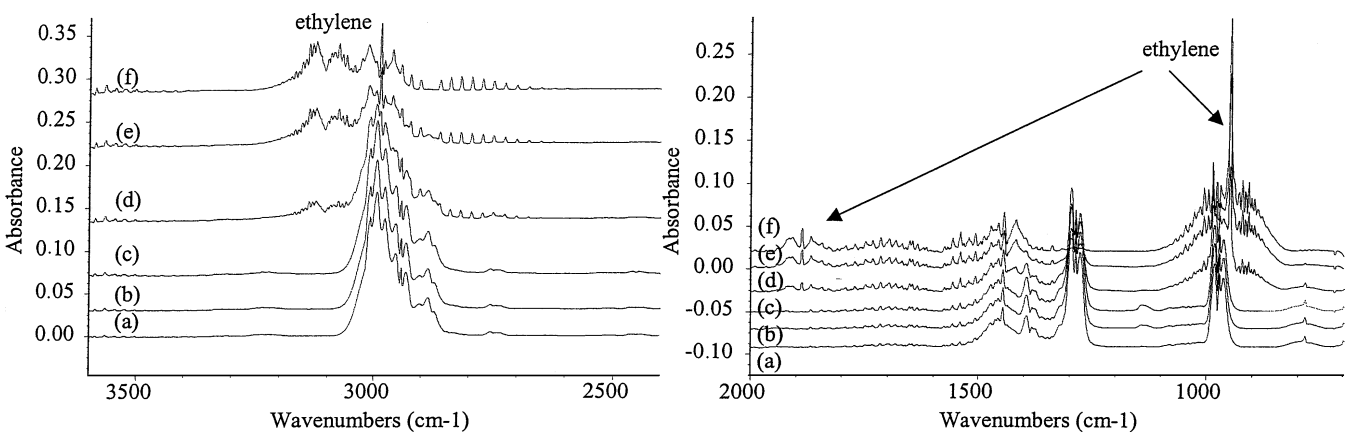

FIG. 1. Gas phase FT-IR spectra corresponding to contact between Al_2O_3 and ethyl chloride at 423 K (a), 473 K (b), 523 K (c), 573 K (d), 573 K for 40 min (e), and 623 K (f).

TABLE 4

Position of the IR and Raman Bands (cm^{-1}) of Ethylchloride Species

Mode	Sym	Assignment	IR gas (5)	Raman liquid (5)	Adsorbed on Al_2O_3	Adsorbed on Al_2O_3/Cu 9%
$\nu 12$	a''	$\nu_{as}CH_2$	3014	3013		3020
$\nu 13$	a''	νCH_2	2986	2978	2983	2983
$\nu 1$	a'	$\nu_s CH_2$		2967	2978	
$\nu 2$	a'	νCH_3	2946	2934	2937	2937
		$1453 + 1470$		2913	2909	
		2×1453	2904	2889		
$\nu 3$	a'	$\nu_s CH_3$	2887	2883	2883	2885
			2875			
				2867		
		$1453 + 1379$[a]				2834
			2747	2737		
$\nu 4$	a'	$\delta_{as}CH_3$	1470			
$\nu 5, \nu 14$	$a'\,a''$	$\delta CH_2, \delta_{as}CH_3$	1448	1453	1451	1450
$\nu 6$	a'	$\delta_s CH_3$	1385	1383	1382, 1395	1382
			1322			
		$974 + 336$[a]				1302,
$\nu 7$	a'	CH_2 wag	1289	1283	1303, 1286	1284
$\nu 15$	a''	CH_2 twist	1251	1248	1250	1250
$\nu 8$	a'	CH_3 rock	1081	1072	1075	1075
$\nu 16$	a''	CH_2 rock	1041, 1030			
$\nu 9$	a'	νC–C	974	969	obscured	obscured
$\nu 17$	a''	CH_3 rock	785		obscured	obscured
$\nu 10$	a'	νC–Cl	677	659	obscured	obscured

[a] Solid CH_3CH_2Cl, 100 K.

species. In particular, a couple of weak bands at 1570 and 1472 cm^{-1} are formed. These bands do not disappear by outgassing, showing that they are due to strongly adsorbed species. They are assigned, in agreement with results of acetic acid adsorption experiments, to the asymmetric and symmetric –COO stretching of acetate species (10). A band is also observed at 1620 cm^{-1} likely due to adsorbed water.

In the higher frequency range (Fig. 2, left) the sharp bands below 3000 cm^{-1}, due to the stretchings of CH_3 and CH_2 groups, can be assigned to ethoxy groups and adsorbed ethylchloride. These bands disappear above 523 K, according to the desorption of EtCl and the decomposition of ethoxy groups.

As always, the interaction causes the perturbation of the surface hydroxy groups of alumina. This results in negative bands in the subtraction spectra between 3800 and 3600 cm^{-1} and in the formation of a broad band between 3600 and 3500 cm^{-1}, due to H-bonded OHs. This feature is

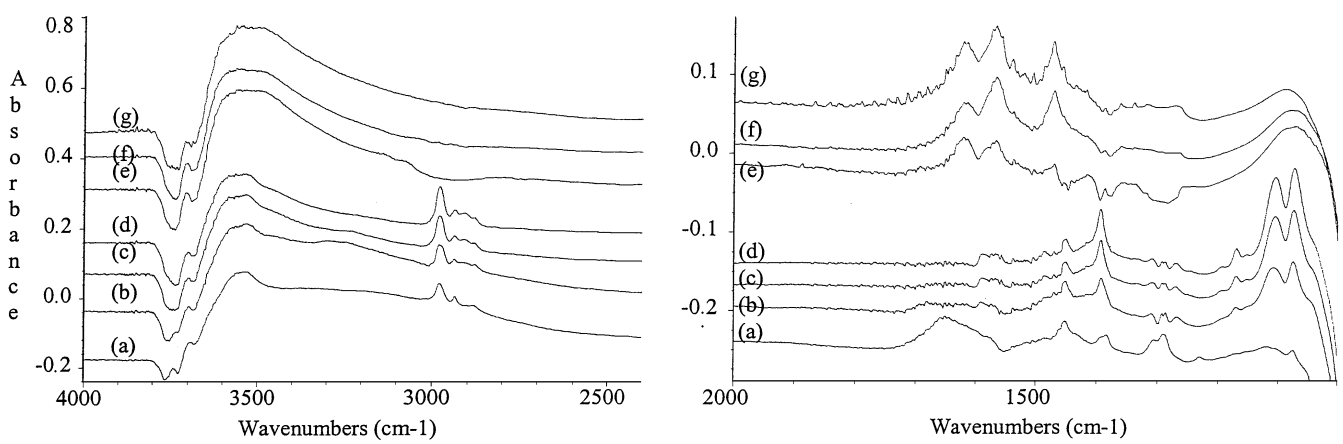

FIG. 2. FT-IR subtraction spectra of the adsorbed species arising from ethylchloride adsorption over Al_2O_3 at room temperature (a), 423 K (b), 473 K (c), 523 K (d), 573 K (e), 623 K (f), and after heating and outgassing at 623 K (g).

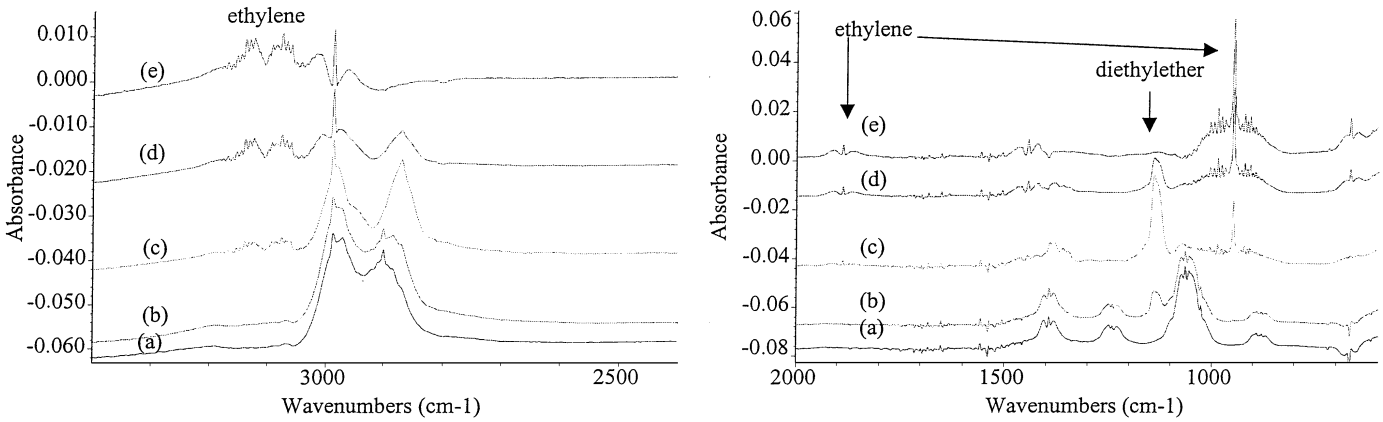

FIG. 3. Gas phase FT-IR spectra corresponding to contact between Al_2O_3 and ethanol at room temperature (a), 423 K (b), 523 K (c), 573 K (d), and 623 K (e).

apparently complex and, by outgassing at increasing temperatures, shows more pronounced a shoulder at 3530 cm^{-1}.

4. *Interaction and Conversion of Ethanol on γ-Al_2O_3: In Situ IR Study*

We also investigated the interaction of the alumina support with ethanol under the same conditions described for EtCl, in order to confirm the attributions proposed for the reaction product formed by ethylchloride interaction. The spectra of the gas in contact with the catalyst at increasing temperatures are reported in Fig. 3. At room temperature only the features of gas-phase ethanol are observed (C–H stretchings at 3000–2800 cm^{-1}, CH_3 deformation at 1395 cm^{-1}, C–O H deformation at 1240 cm^{-1}, C–O and C–C stretching at 1060 and 1029 cm^{-1} (11)). Additional bands at 1142 cm^{-1} (with a shoulder at 1130 cm^{-1}), assigned below, and at 2870 cm^{-1} (in the C–H stretching region) are observed weak at 423 K and stronger at 523 K and later decrease in intensity, disappearing at 623 K. Starting from 523 K gaseous ethylene (bands at 1888 and 950 cm^{-1}) is observed (note that the bands of gas-phase water have been subtracted in the spectrum).

In Fig. 4 the spectra of the corresponding surface species are reported. At RT the strong complex of bands in the 1200–1000 cm^{-1} region due to coupled C–O and C–C stretchings, where we can distinguish the bands of ethoxides at 1167 (weak), 1120, and 1075 cm^{-1} together with the corresponding CH deformation bands at 1447 and 1388 cm^{-1} (stable up to 573 K) are evident (8, 9). Undissociatively adsorbed ethanol is characterized by the band at 1060 cm^{-1}, and is almost totally desorbed (or dissociated) at 423 K.

The ethoxide bands disappear almost completely at 623 K when weak bands at 1580 and 1470 cm^{-1}, due to surface acetates, are observed.

The data described in this section fully confirm that ethoxide species can be produced both by ethanol (by dissociative adsorption) and by EtCl (by nucleophilic substitution by an oxide anion) and are intermediates in the production of ethylene by an elimination reaction (12).

However, acetate species are also observed to form from ethanol like from EtCl on alumina. It has already been reported long ago in the literature that carboxylate species can be produced from alcohols on alumina, namely acetates from ethanol (8). They probably form via dehydrogenation, with hydroxide groups acting as oxygen atom donors. This mechanism implies that one hydroxy group per ethoxide group is consumed upon this process.

In order to confirm our hypothesis about oxygenate compound formation from ethylchloride interaction with the catalyst, we also studied the interaction of diethylether on alumina at room temperature (Fig. 5) both in the presence of gas phase ether (5 Torr) and after evacuation. The IR spectrum of diethylether vapor (Fig. 5c) shows a very prominent band at 1145 cm^{-1}, due to the asymmetric C–O–C stretching (13). This band perfectly corresponds to that observed strong in the spectra of the gas phase species

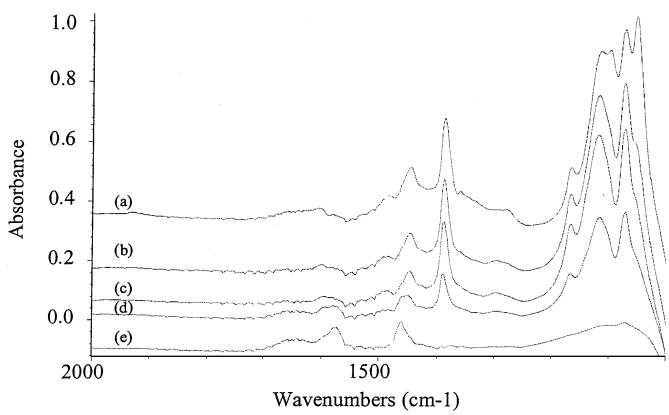

FIG. 4. FT-IR subtraction spectra of the adsorbed species arising from ethanol adsorption on Al_2O_3 pressed disks at room temperature (a), 423 K (b), 473 K (c), 523 K (d), and 623 K (e).

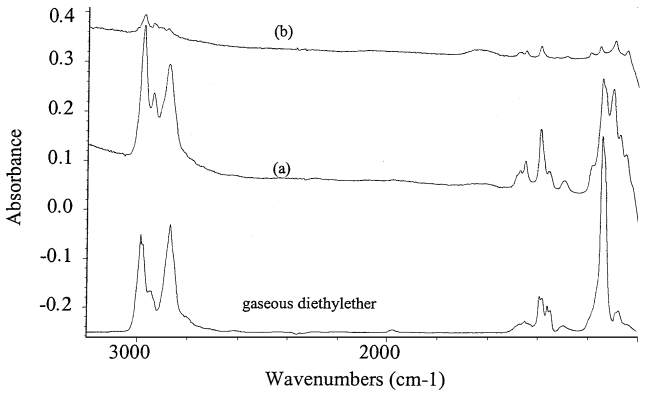

FIG. 5. FT-IR subtraction spectra of the adsorbed species arising from diethyl ether adsorption on Al_2O_3 pressed disks in the presence of diethyl ether (a), and after successive outgassing at room temperature (b).

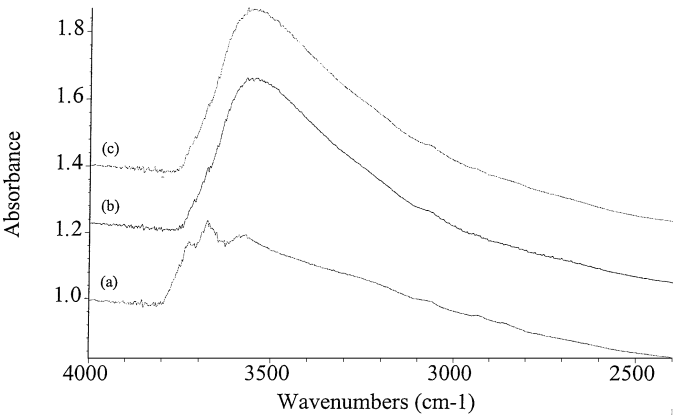

FIG. 6. FT-IR spectra of Al_2O_3 after activation at 523 K (a), after contact with HCl at 523 K (b), and after contact with HCl at 523 K and brief outgassing (c).

arising from ethanol contact with Al_2O_3 (Figs. 3b and 3c) and weak in the spectra of the gas phase species arising from EtCl contact with Al_2O_3 (Figs. 1b and 1c). The spectrum of the adsorbed species arising from contact of alumina with diethylether vapor closely corresponds to that of the vapor. After outgassing, some bands decrease in intensity more than others (in particular the CH deformation modes between 1300 and 1450 cm^{-1} are strongly decreased in intensity), while the bands in the region 1200–1000 cm^{-1} are shifted, slightly but significantly, to 1193, 1153, 1093, and 1045 cm^{-1}. The positions correspond closely to those observed for the Lewis acid–base complex $(C_2H_5)_2O$–$AlCl_3$ (14), and this suggests that a coordination bond between an ether oxygen lone pair and Lewis acid sites of alumina occurs. These data confirm that the weak components between 1200 and 1000 cm^{-1} (namely at 1190, 1151, and 1100 cm^{-1}) observed in the spectra of the adsorbed species arising from EtCl and ethanol are actually due to adsorbed diethylether, although they can be partially superimposed to bands of the surface alkoxide species (see Table 5).

5. *Effect of the Chlorination of Alumina on the Interaction and Dehydrochlorination of EtCl*

HCl is obviously present in the feed of oxychlorination reactors and is the product of dehydrochlorination process.

TABLE 5

IR Bands Due to Adsorbed Species Arising from EtCl and EtOH Interaction with Al_2O_3 Surface (in cm^{-1})

	Adsorbed species				
Adsorbate	$(Et)_2O$ ads	EtO^-	$(Et)_2O$ ads	$(Et)_2O$ ads	EtO^-
EtCl	1192	1167	1151	1103	1073
EtOH		1167		1120	1075
Et_2O	1193		1153	1093	

For this reason, we wanted to follow the effects of HCl presence in the reaction under study. In Fig. 6, the spectra of the surface hydroxy groups of alumina after activation by outgassing at 523 K and after chlorination with HCl at the same temperature followed by brief outgassing, are reported. The bands of the free surface OHs of alumina in the range 3800–3650 cm^{-1} are almost disappeared after treatment with HCl, while a broad band centered at near 3550 cm^{-1} is observed. By monitoring the gas-phase upon heating of HCl-treated alumina, it is evident that HCl gas is released from alumina already at 423 K. It is thus concluded that the adsorption of HCl on alumina is at least partially reversible in the range typical for the oxychlorination reaction even if up to 523 K (the highest temperature in this range) the alumina surface can be still partially covered by chlorine ions (15).

Consequently, it seems reasonable to conclude that the actual extent of chlorination of alumina depends on the temperature (as already stated in the literature on the subject (15, 16)) and on the HCl pressure as well.

In Fig. 7 the spectra of the surface species arising from the interaction of EtCl with previously chlorinated alumina are reported. After adsorption of EtCl on such a surface the bands of adsorbed EtCl are found, near 1450, 1380, and 1280 cm^{-1}. However, traces of a doublet, 1095 and 1070 cm^{-1}, are already found at RT and become quite strong at 473 K. As demonstrated previously, these bands are due to the C–O and C–C stretchings of ethoxy species formed through the nucleophilic substitution by oxide anions on the adsorbed EtCl. The comparison of the spectrum of Fig. 7b with that of Fig. 2c shows that a small decrease in the ethoxy group/EtCl adsorbed species ratio results from surface chlorination with HCl. At the same time the complex band at 1290 cm^{-1} (due to adsorbed EtCl) is clearly evident, indicating the interaction at the surface of undissociated ethylchloride.

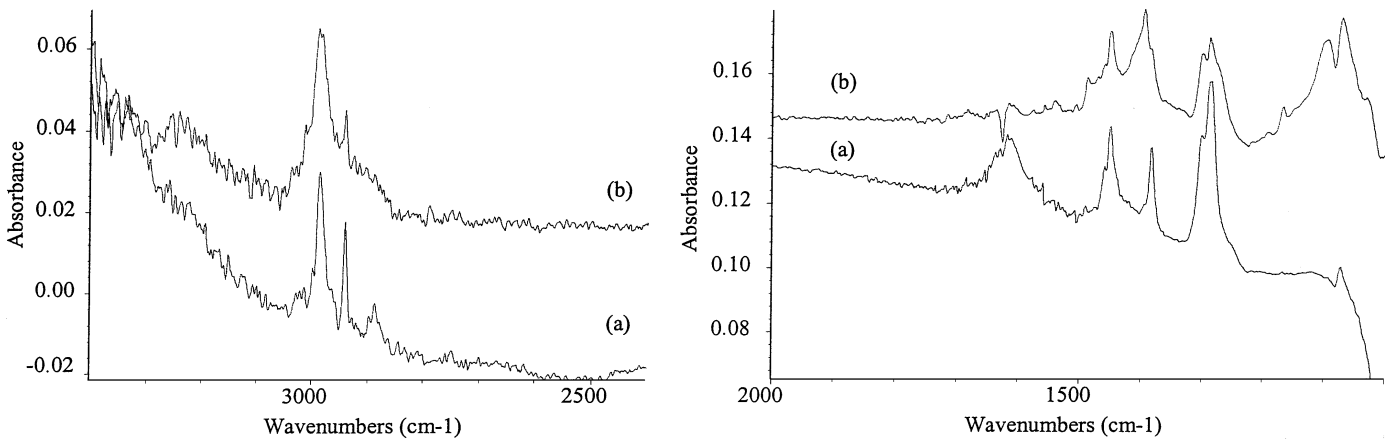

FIG. 7. FT-IR subtraction spectra of the surface species arising from ethyl chloride adsorption over Al_2O_3 pretreated with HCl at room temperature (a) and at 473 K (b).

The intensity of the bands of ethoxides rises a maximum at 473 K and these bands are still present at 523 K, being almost disappeared at 573 K, on previously chlorided alumina. At this temperature the typical features of gas phase ethylene and HCl are almost absent. They appear and become very intense at 573 K, showing again the elimination reaction of ethoxide species. Bands due to carboxylate species are less intense than in the absence of HCl treatment, even at 573 K.

It seems likely that HCl pretreatment hinders the alkoxy groups formation (and, as a consequence, of acetate formation) at the surface of pure alumina. However, this only slightly affects the final elimination reaction to give unsaturated product and HCl, possibly because $AlCl_3$-type sites can also give rise to dehydrochlorination directly, without the intermediacy of ethoxide groups.

6. Interaction and Conversion of EtCl on γ-Al_2O_3/$CuCl_2$ (1% Cu)

The spectra obtained under the same conditions as in Figs. 1 and 2 on the catalyst with 1 CuA are qualitatively completely consistent with what occurs on pure alumina. Even at an higher temperature (523 K) the adsorbed species are constituted by the alkoxides (bands in the region near 1100 cm^{-1}). We likely observe here the reactivity of the residually exposed alumina surface, rather than the activity, if any, of the copper chloride species.

7. Interaction and Conversion of EtCl on γ-Al_2O_3/$CuCl_2$ (9% Cu)

The interaction of ethyl chloride with 9 CuA at temperatures below 473 K gives similar results, but with some important differences (Fig. 8) with respect to the pure alumina and also to the catalyst with 1 CuA. Until 373 K the ethyl chloride adsorption is mostly nonreactive, while alkoxides become predominant at 473 K; starting from this temperature we observe the growth of a couple of intense bands near 1590 and 1440 cm^{-1}, assigned to acetate species. Acetic acid adsorption over the same surface supports our assignment. Thus in the presence of $CuCl_2$ alkoxy ions are formed more slowly than on the pure alumina, and can also be oxidized extensively to acetates most probably by the copper ions, that are consequently reduced.

We can remark that we previously reported (3) that $CuCl_2$ "neutralizes" the nucleophilic oxygen species of alumina involved in the reactive adsorption of CO_2 to give carbonates. The same nucleophilic oxide species are likely involved in the nucleophilic substitution giving rise to ethoxy groups from EtCl on alumina. These data suggest that the impregnation with $CuCl_2$ does not cause a total neutralization of these sites. On the other hand, our previous data showed that also on the $CuCl_2/\gamma Al_2O_3$ (9% Cu) catalyst the alumina support is still in part uncovered. The less

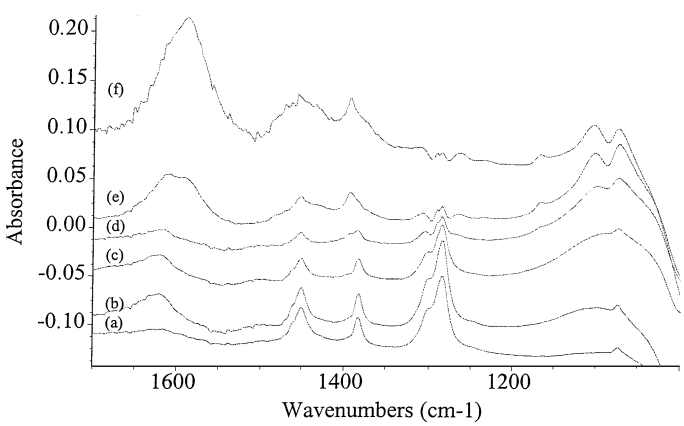

FIG. 8. FT-IR subtraction spectra of the surface species arising from ethyl chloride adsorption over Al_2O_3/Cu 9% disk at room temperature (a), after 15 min at room temperature (b), 373 K (c), 423 K (d), 473 K (e), and 523 K (f) in the presence of the gas. The gaseous ethyl chloride has been automatically subtracted.

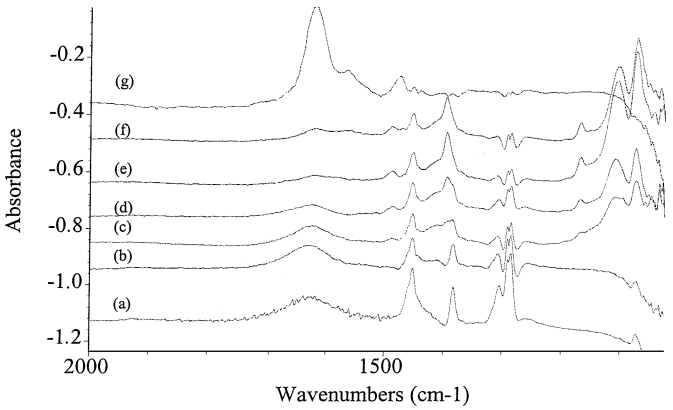

FIG. 9. FT-IR subtraction spectra of the surface species arising from EtCl adsorption over the catalyst $Al_2O_3/MgCl_2$ at room temperature (a), 373 K (b), 423 K (c), 473 K (d), 523 K (e), 573 K (f), and 623 K (g). The gaseous EtCl has been automatically subtracted.

active nucleophilic sites are probably still available, but they act at higher temperatures.

On the other hand, our data do not exclude that $CuCl_2$ centers and $AlCl_3$-type sites can also be active in the dehydrochlorination of EtCl without the intermediacy of alkoxides.

8. Interaction and Conversion of EtCl on $MgCl_2$- and KCl-Doped Aluminas

By analogy with the experiments performed over alumina we also performed experiments of conversion of EtCl and monitoring of the gas phase over $MgCl_2$- and KCl-doped aluminas. In Figs. 9 and 10 the spectra of the adsorbed species observed upon conversion of EtCl over $MgCl_2$–Al_2O_3 and KCl–Al_2O_3 are reported, respectively. On $MgCl_2$–Al_2O_3, at the beginning the spectra show the sharp bands of adsorbed EtCl (CH deformations in the regions near 1450, 1380, 1305, and 1285 cm^{-1}) and then

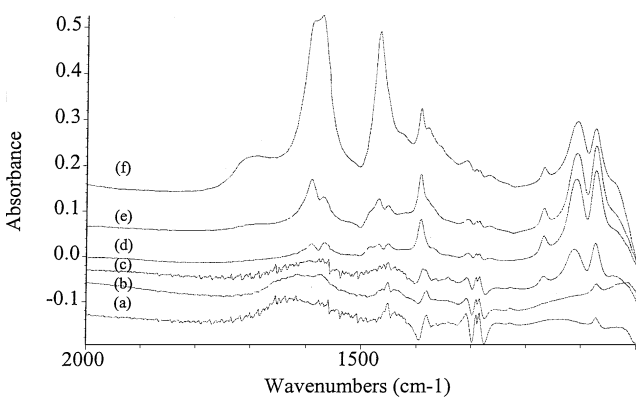

FIG. 10. FT-IR subtraction spectra of the surface species arising from EtCl adsorption over the catalyst Al_2O_3/KCl at room temperature (a), 373 K (b), 473 K (c), 523 K (d), 573 K (e), and 623 K (f). The gaseous EtCl has been automatically subtracted.

the progressive growth of the C–O/C–C stretching bands of ethoxides (1150–1050 cm^{-1} region). These bands grow up to 523 K, slightly decrease between 523 and 573 K, and disappear completely at 623 K. Simultaneously, the gas phase spectra show the bands of gaseous ethylene starting from 573 K. Again, simultaneously, also the rotovibrational spectrum of gas-phase HCl appears. Only at 623 K do bands assignable to acetate species appear in the surface spectrum. So the chemistry observed over $MgCl_2$–Al_2O_3 is strictly similar to that observed on pure Al_2O_3, although the ethoxide stability seems to be slightly enhanced by $MgCl_2$.

In the case of KCl–Al_2O_3 again we found on the surface the formation of ethoxide species bands in the 1150–1050 cm^{-1} region at least starting from 473 K (Fig. 10). However, these species do not decompose at all up to 623 K. Correspondingly, no HCl and no ethylene are observed in the gas phase up to this temperature. This behavior and very small shifts in the spectrum of ethoxide species suggest to us that in this case ethoxide can be bonded to K^+ ions, much less acidic than Al^{3+} and/or Mg^{2+}. This can lower the polarization of the C–O bond of ethoxides, thereby preventing their decomposition up to 623 K. On the other hand, the by-reaction giving rise to acetates is not hindered by KCl. In fact, strong bands of acetates are observed at 623 K (Figs. 11e and 11f).

9. An FT-IR Study of the Conversion of EtCl over $MgCl_2$- and KCl-Doped $CuCl_2$–Al_2O_3 Catalysts

The behavior of the $MgCl_2$- and KCl-doped $CuCl_2$–Al_2O_3 catalysts are, qualitatively, very similar to those observed on the corresponding supports, $MgCl_2$- and KCl-doped alumina, discussed above. The only evident difference is that stronger bands of acetate species are also found at the surface, similar to those observed on $CuCl_2$–Al_2O_3 catalysts. This provides evidence for a typical oxidizing reactivity of cupric centers.

The comparison of the results obtained with CuA, KCuA, and MgCuA samples shows that $MgCl_2$ slightly increases the stability of ethoxides while KCl strongly increases their stability.

DISCUSSION

1. On the Dehydrochlorination of EtCl

The above data show that alumina is highly active in the dehydrochlorination of EtCl to ethylene + HCl. The IR data demonstrate the occurrence of the reaction mechanism shown in Scheme 1. On the other hand, the desorption of HCl following (formally)

$$^{-}OH + Cl^{-} \rightarrow O^{=} + HCl$$

closes a reasonable catalytic cycle for the reaction from EtCl to ethylene on pure alumina, restoring the active site

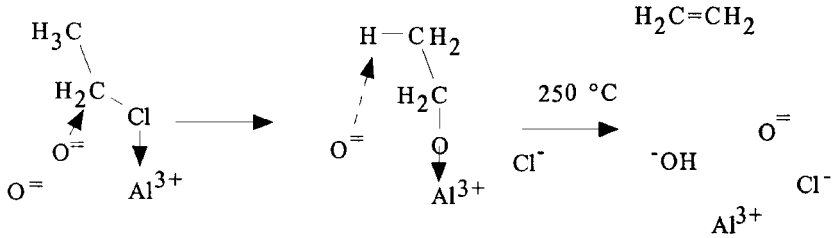

SCHEME 1. Production of ethylene from EtCl on pure alumina.

necessarily constituted by a Lewis acidic coordinatively unsaturated Al^{3+} cation coupled with two oxide anions exposed at the surface. It seems evident, that hydrochloric acid can inhibit this mechanism because it can interact with the same catalytic site. In effect, our study concerning HCl/alumina interaction suggests that HCl can actually interact with the Lewis acid sites of alumina. On the other hand, it seems that this inhibition by HCl is only partial and reversible. However, it is possible that on chlorided alumina (alumina pretreated with HCl) another additional mechanism is activated, without the intermediacy of alkoxide (Scheme 2).

It is reasonable to suppose that this way is slower than that via alkoxide, because the chloride anion is a weaker base than the oxide anion and should be less active in abstracting the proton. We also obtained an indication that acetate species are formed by high-temperature evolution of the surface alkoxide on alumina. They can represent precursors for coke if the elimination reaction is carried out in the absence of oxygen.

On the other hand, $CuCl_2$ centers (which carry significant Lewis acidity (3)) can also be active in the direct dehydrochlorination of EtCl.

A by-reaction occurring during this process is the nucleophilic substitution of ethoxy groups on ethylchloride giving rise to diethylether (Scheme 3).

Our data indicate that the treatment with HCl and also the presence of Cu, K, and Mg chloride species at the alumina surface more or less hinder the dehydrochlorination reaction. This occurs either by reducing the number and/or the reactivity of the surface oxide species involved in the conversion of EtCl into ethoxy groups (this seems to occur for treatment with HCl and by the presence of $CuCl_2$), or by stabilizing these ethoxy groups as less reactive forms (this seems to occur mainly for catalysts doped with KCl or MgCl).

On the other hand, it seems that the data (both IR and pulse reactivity data) can be interpreted assuming that the site reactivity scale for EtCl to ethylene is the following:

$$\text{bare } Al_2O_3 > CuCl_2 \text{ on } Al_2O_3 > MgCl_2 \text{ on } Al_2O_3 > KCl \text{ on } Al_2O_3.$$

As for the Cu-containing catalysts, by combining the above site reactivity scale the dehydrochlorination activity apparently follows the trend

$$CuCl_2 \text{ on } Al_2O_3 > MgCl_2\text{–}CuCl_2 \text{ on } Al_2O_3 \gg KCl\text{–}CuCl_2 \text{ on } Al_2O_3.$$

So it seems likely that on $CuCl_2$–Al_2O_3 and on $MgCl_2$-doped $CuCl_2$–Al_2O_3 the support is acting as the catalyst for EtCl dehydrochlorination, while on KCl-doped $CuCl_2$–Al_2O_3 $CuCl_2$ is likely acting as the catalyst for EtCl dehydrochlorination.

The pulse reactor studies suggest that the most active alumina sites are actually destroyed already at the lowest $CuCl_2$ coverages of 1 CuA. Previous CO_2 adsorption experiments actually showed that, in spite of the very low theoretical monolayer coverage of this sample (9%), 31% of the CO_2 adsorbing sites (obviously, the strongest ones) are already destroyed. The activity of $CuCl_2$-type sites too in dehydrochlorination justifies the almost identical conversion of EtCl, measured on surface area basis, on the three undoped CuA samples. In fact, the activity of the increasing $CuCl_2$-type sites can balance the loss of the weakest alumina sites by increasing Cu loading.

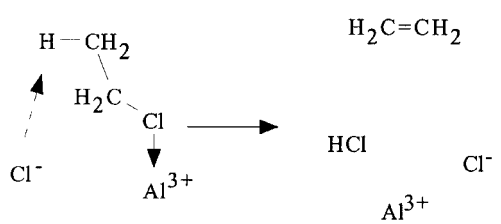

SCHEME 2. Possible way of producing ethylene from EtCl on heavily chlorided alumina.

2. Relevance with Respect to the Ethylene Oxychlorination Process

Our previous data showed that uncovered alumina can be still exposed on active $CuCl_2$–Al_2O_3 oxychlorination catalysts (3). The present data show that this uncovered support surface can act as a dehydrochlorination catalyst. The desired product of the dehydrochlorination process, i.e., dichloroethane, can actually undergo dehydrochlorination,

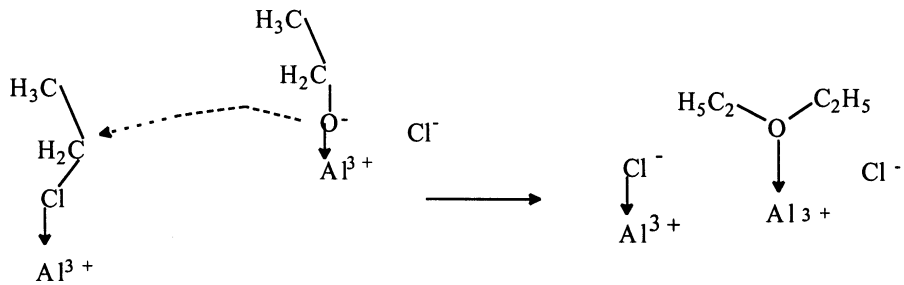

SCHEME 3. Production of diethylether from EtCl on pure alumina via ethoxy groups.

giving rise to vinyl chloride monomer (VCM) which is an undesired product. In fact, VCM can be oxychlorinated to 1,1,2-trichloroethane in the oxychlorination reactor.

Our data suggest that doping $CuCl_2$–Al_2O_3 oxychlorination catalysts with $MgCl_2$ and, mainly, KCl has the beneficial effect of reducing the dehydrochlorination activity, so increasing the selectivity to EDC and decreasing the production of VCM and of its following oxychlorination products. So, part of the beneficial effect of such dopants is, more than influencing the $CuCl_2$ active sites, in poisoning the unwanted activity of the alumina support.

REFERENCES

1. Naworski, J. S., and Velez, E. S., *in* "Applied Industrial Catalysis" (B. E. Leach, Ed.), Vol. 1. Academic Press, New York, 1983.
2. Newmann, M. N., *Encyclopedia Polymer Sci. Eng.* **17**, 245 (1985).
3. Finocchio, E., Rossi, N., Busca, G., Padovan, M., Leofanti, G., Cremaschi, B., Marsella, A., and Carmello, D., *J. Catal.* **179**, 606 (1998).
4. Finocchio, E., Busca, G., Ramis, G., and Lorenzelli, V., *in* "Oxidation Catalysis" (R. K. Grasselli, T. Oyama, A. M. Gaffney, and J. E. Lyons, Eds.), p. 989. Elsevier, Amsterdam, 1997.
5. Miller, F. A., and Kiviat, F. E., *Spectrochim. Acta* **25**, 1363 (1969); McKean, D. C., McQuillan, G. P., Robertson, A. H. J., Murphy, W. F., Mastryukov, V. S., and Boggs, J. E., *J. Phys. Chem.* **99**, 8994 (1995).
6. Arnett, R. L., and Crawford, B. L., *J. Chem. Phys.* **18**, 118 (1953); Knippers, W., Vanelvohort, K., Stolte, S., and Reuss, G., *Chem. Phys.* **98**, 1 (1985).
7. Hertzberg, G., "Molecular Spectra and Molecular Structure. 1. Spectra of Diatomic Molecules." Van Nostrand, Princeton, NJ (1950).
8. Greenler, R. G., *J. Phys. Chem.* **37**, 2094 (1962).
9. Jeziorowski, H., Knözinger, H., Meye, W., and Muller, H. D., *J. Chem. Soc. Faraday Trans I* **69**, 1744 (1973).
10. Nakamoto, K., "Infrared and Raman Spectra of Inorganic and Coordination Compounds." Wiley and Sons ed., New York, 1986.
11. Lin-Vien, D., Colthup, N. B., Fateley, W. G., and Grasselli, J. G., *in* "The Handbook of Infrared and Raman Characteristic Frequencies of Organic Molecules." Academic Press, San Diego, 1991.
12. Pine, H., and Manassen, J., *Adv. Catal.* **16**, 49 (1976).
13. Wieser, H., Laidlaw, W. G., Krueger, P. J., and Fuhrer, H., *Spectrochim. Acta* **24**A, 1055 (1968).
14. Olah, G. A., *in* "Friedel Crafts and Related Reactions," Vol. 1, p. 700. Interscience, New York, 1963.
15. Arena, F., Frusteri, F., Mondello, N., Giordano, N., and Parmaliana, A., *J. Chem. Soc. Faraday Trans.* **88**, 3353 (1992).
16. Kytokivi, A., Lindblad, M., and Root, A., *J. Chem. Soc. Faraday Trans.* **91**, 941 (1995).